ASM | Applied and Environmental Microbiology

Check for updates

| Environmental Microbiology | Full-Length Text

Anaerobic microorganisms alter heavy oil chemistry by oxygenation and sulfurization

Mourad Harir,[1,2] Mark Pannekens,[3] Lisa Voskuhl,[3] Verena Brauer,[3] Philippe Schmitt-Kopplin,[1,2] Rainer U. Meckenstock[3]

AUTHOR AFFILIATIONS See affiliation list on p. 14.

ABSTRACT Microbial transformation of heavy oil under anoxic conditions involves complex changes in hydrocarbon and heteroatom-containing molecular compositions. However, the molecular-level evolution of sulfur-containing compounds and their relationship to hydrocarbon transformation remain insufficiently resolved. In this study, long-term anaerobic microcosms containing heavy oil from Pitch Lake, Trinidad and Tobago, were analyzed using Fourier transform ion cyclotron resonance mass spectrometry (FT-ICR MS) and microbial community profiling to evaluate temporal changes in molecular compositions and microbiota structure over 945 days of incubation. FT-ICR MS detected 4,499 molecular formulas dominated by CHO-, CHNO-, CHOS-, and CHNOS-class formulas. Pronounced compositional shifts occurred during incubation, with sulfur-containing molecular formulas becoming increasingly abundant and resulting in a marked increase in CHOS-class formulas over time. Intensity-weighted elemental formulas showed increasing oxygen and sulfur abundances, while the average *m/z* increased from 344 at day 93 to 366 at day 945, corresponding to an approximately 6.4% increase in the intensity-weighted average molecular mass. Multivariate analyses revealed distinct temporal clustering of samples and parallel shifts in microbial community composition, depicting a greater contribution of anaerobic and sulfur-associated taxa. Correlation analyses further showed associations between microbial community shifts and increasing abundances of oxidized sulfur-containing compounds, particularly $CHSO_3$- and $CHSO_4$-class formulas. These findings indicate substantial reorganization of the heteroatom-containing molecular pool during anoxic incubation and highlight the potential roles of microbial and sulfur-related processes in the transformation of heavy oil under anoxic conditions.

IMPORTANCE Heavy oil reservoirs contain complex mixtures of hydrocarbons and heteroatom-containing compounds that undergo transformation under anoxic conditions. Characterizing the molecular-level changes occurring during these transformations is important for understanding hydrocarbon biodegradation, the persistence of recalcitrant compounds, and the formation and fate of organic sulfur species in oil reservoirs. Using Fourier transform ion cyclotron resonance mass spectrometry (FT-ICR MS) and microbial community analyses, this study reveals that long-term anaerobic incubation drives enrichment of CHOS-class formulas, reduced microbial diversity, and shifts toward anaerobic, sulfur-associated taxa. These findings demonstrate that microbial and sulfur-driven processes play a key role in reorganizing oil chemistry and suggest that co-metabolic activity contributes to the accumulation of partially transformed sulfur-containing compounds. By directly linking changes in microbial community composition with ultrahigh-resolution molecular characterization, this work provides important new insights into the microbial and chemical mechanisms controlling heavy oil transformation and sulfur metabolism in subsurface oil reservoirs.

KEYWORDS anaerobic microcosms, FT-ICR MS, oxygenation/sulfurization, Pitch Lake oil

Editor Jennifer B. Glass, Georgia Institute of Technology, Atlanta, Georgia, USA

Address correspondence to Rainer U. Meckenstock, rainer.meckenstock@uni-due.de, or Mourad Harir, mourad.harir@helmholtz-munich.de.

The authors declare no conflict of interest.

See the funding table on p. 15.

Received 23 June 2026
Accepted 28 September 2026
Published 27 October 2026

Copyright © 2026 Harir et al. This is an open-access article distributed under the terms of the Creative Commons Attribution 4.0 International license.

Downloaded from https://journals.asm.org/journal/aem on 04 November 2026 by 2a02:2455:1ca1:2600:a7cd:7757:1758:28a8.

Downloaded from https://journals.asm.org/journal/aem on 04 November 2026 by 2a02:2455:1ca1:2600:a7cd:7757:1758:28a8.

Most of the world's oil reservoirs are affected by microbial degradation, leading to heavier, more viscous oil with reduced economic value (1). A major portion of oil degradation in reservoirs occurs at the oil-water interface, located beneath the oil leg, the hydrocarbon-bearing zone of the reservoir (2). Microorganisms inhabit the water-filled pore spaces of the underlying aquifer or water leg and may utilize hydrocarbons as carbon and electron sources following their dissolution into the aqueous phase. Hydrocarbon biodegradation is coupled to the reduction of available electron acceptors such as dissolved nitrate, sulfate, or methanogenesis. Hot spots of biodegradation in reservoirs have been identified by gas chromatography analysis of oil composition. Distinct gradients in alkane content, with less degraded oil at the top and more heavily degraded oil at the bottom of reservoirs, indicate that most biodegradation occurs at the oil-water interface (2). Analyses of oil samples, including those from natural oil seeps in Trinidad and California (USA) (3), further suggest that microorganisms may also inhabit small water-filled voids within the oil phase, extending the potential zone of biodegradation into the oil leg (2, 4–6).

A key challenge in microbial hydrocarbon degradation is the low water solubility of hydrocarbons, which limits their bioavailability (6). While microbial interactions are essential, degradation rates are strongly influenced by physical factors, particularly the extent of oil-water contact that governs hydrocarbon transfer into the aqueous phase (6, 7). In oil reservoirs, microbial activity is therefore concentrated at this interface. In the presence of nutrients, microorganisms can form biofilms on oil or bitumen surfaces. Such biofilms, composed primarily of fermentative and sulfate-reducing bacteria, have been observed on bitumen under near-natural conditions (6). These biofilms retain surfactants and extracellular enzymes, reducing diffusion limitations and facilitating hydrocarbon access. Over time, microbial activity at such interfaces transforms oil into more bioavailable compounds. Bitumen also contains microscopic water droplets that host oil-degrading microorganisms, potentially enhancing degradation by increasing the interfacial area (3–5). These droplets may additionally provide protective microenvironments that support microbial survival under extreme reservoir conditions.

Although crude oil contains a wide range of heteroatom-bearing compounds, sulfur-containing organic compounds are of particular importance because their formation and transformation influence the molecular composition and long-term preservation of organic matter. Biosynthesis, early diagenetic formation, and reactions between hydrocarbons and reduced inorganic sulfur species, particularly sulfide and polysulfides, have been proposed as major pathways for sulfur incorporation into organic matter (8–15). Sulfur incorporation depends on organic matter quality, but the process is complex, rapid, and not fully understood (16–18). Diagenetic sulfur incorporation has been suggested to preserve biolipids and inhibit biodegradation of algal-derived organic matter (11, 14, 19). In addition, sulfurization of highly reactive unsaturated compounds has been reported (12, 20), and abiotic sulfurization is widely considered a dominant mechanism for organic sulfur compound formation under anoxic conditions (21). Prominent sulfur-containing compounds in crude oil include aromatic thiophenes, while nitrogen is commonly present in quinoline and carbazole structures. However, a wide diversity of heteroatom-containing compounds is also detected in oil and water phases, with sulfur being the most abundant heteroatom.

Fourier transform ion cyclotron resonance mass spectrometry (FT-ICR MS) analyses of water droplets in heavy oil have revealed diverse O-, S-, and N-containing aliphatic and aromatic molecules (4), some resembling known anaerobic polycyclic aromatic hydrocarbon (PAH) degradation products, suggesting *in situ* biodegradation. Although oxidized compounds may be more reactive than hydrocarbons, sulfur-containing CHOS compounds can persist as metabolic end products. In this study, we analyzed temporal shifts in CHO-, CHNO-, CHOS-, and CHNOS-class formulas during anoxic microbial incubation and related these changes to microbial community composition. We hypothesize that chemical diversity arises from co-metabolism, whereby microorganisms transform or degrade compounds that are not necessarily used as primary

growth substrates while utilizing other compounds as carbon and electron sources for growth. We incubated microcosms containing heavy oil, native microorganisms, and artificial medium for 945 days. FT-ICR MS was used to determine molecular formulas, and previously obtained microbial community data (6) were reanalyzed to investigate associations with heteroatom-containing compound production. These long-term anoxic incubations provide a laboratory model that simulates key aspects of the progressive microbial transformation of crude oil under anoxic conditions in subsurface oil reservoirs over time.

Downloaded from https://journals.asm.org/journal/aem on 04 November 2026 by 2a02:2455:1ca1:2600:a7cd:7757:1758:28a8.

MATERIALS AND METHODS

Microcosm experiment on heavy oil incubation

This study used the same heavy-oil microcosm incubations described previously (6). Briefly, 250-mL glass flasks were filled with 60–30 g of heavy oil and 140 mL of a brackish water medium formulated based on the geochemical composition of naturally occurring oil-associated water. Based on the mean heavy-oil mass of 104.97 g and an oil density of 1.15 g mL^{-1}, the corresponding oil volume was approximately 91.28 mL, resulting in an aqueous-medium-to-oil ratio of approximately 1.5:1 (v/v), or 1.3:1 (w/w). The medium contained NaCl, $NaHSO_4$, NH_4Cl, $NaH_2PO_4{\cdot}2H_2O$, KCl, $CaCl_2{\cdot}2H_2O$, and $MgCl_2{\cdot}6H_2O$ at concentrations described in Text S1. The medium was buffered to pH 7.0, with a measured pH of 7.9 after addition to the microcosms. The sealed microcosms contained a nitrogen-flushed headspace and were incubated at approximately 32°C under anaerobic conditions. Water-phase samples were collected from the same incubations at five time points during the 945-day incubation and subsequently analyzed by high-resolution FT-ICR MS at Helmholtz Munich (Germany). The FT-ICR MS measurements therefore provided a complementary molecular-level characterization of chemical changes occurring during the previously established microcosm incubation. Detailed information on microcosm preparation, medium composition, ^{13}C labeling, sampling, and sample handling is provided in Text S1.

Microbial community analysis

Microbial community analysis based on 16S rRNA gene amplicon sequencing was previously reported (3, 6). The sequencing data were obtained from samples collected at 470, 604, and 945 days of incubation and are available in the NCBI database under BioProject PRJNA645080. Further details on the data analysis are provided in Text S2.

High-field FT-ICR mass spectrometry

The water phases from the heavy oil incubation experiment were acidified to pH 2 and desalted using solid-phase extraction (SPE) with Bond Elut PPL cartridges (100 mg, 1 mL, Agilent), containing a styrene-divinylbenzene-based sorbent with a nonpolar surface (22), prior to electrospray infusion (Text S3). Mass spectra were acquired on a 12T Bruker Solarix instrument, with data processed using Compass Data Analysis 4.1. Molecular formulas were assigned using NetCalc (23). Intensity-weighted average values of elemental composition and chemical indices, including O/C, H/C, C/N, C/S, double bond equivalent (DBE), mass-to-charge ratio (*m/z*), and carbon oxidation state (Zc), were determined for the water phases. The standard error of the mean (SEM) was calculated from triplicate analyses and is reported for the elemental compositions, DBE, *m/z*, and Zc values (Table 1). For molecular-level comparison among samples, an inter-sample ranking analysis was performed for molecular formulas commonly assigned to CHOS-containing formulas. Common molecular formulas were identified across the samples, and their relative mass-peak intensities were ranked within each sample to generate a formula-specific inter-sample ranking, following the approach described in (24). This approach enables comparison of the relative distribution of common molecular formulas among samples without implying differences in their absolute concentrations.

Downloaded from https://journals.asm.org/journal/aem on 04 November 2026 by 2a02:2455:1ca1:2600:a7cd:7757:1758:28a8.

TABLE 1 Mean intensity-weighted elemental composition, elemental ratios, DBE, mass-to-charge ratio (*m/z*), and carbon oxidation state (Zc) of mass signals assigned from negative electrospray ionization 12T FT-ICR MS analyses of the water phases of heavy oil from Pitch Lake, Trinidad, during a 945 day incubation[a]

Incubation period (days)	H (atom%)	C (atom%)	O (atom%)	N (atom%)	S (atom%)	O/C	H/C	C/N	C/S	DBE	*m/z*	Zc
93	54.76 ± 0.234	36.68 ± 0.068	7.19 ± 0.139	0.17 ± 0.042	1.18 ± 0.063	0.19	1.49	247.67	31.21	5.50 ± 0.034	344 ± 3.703	−1.048 ± 0.021
140	54.58 ± 0.098	36.70 ± 0.123	7.16 ± 0.132	0.26 ± 0.026	1.27 ± 0.059	0.19	1.48	141.07	28.83	5.90 ± 0.084	365 ± 1.679	−1.020 ± 0.012
470	54.17 ± 0.143	36.33 ± 0.206	7.93 ± 0.081	0.14 ± 0.002	1.40 ± 0.074	0.21	1.49	246.11	25.92	5.40 ± 0.075	348 ± 4.189	−0.978 ± 0.006
604	54.23 ± 0.158	36.15 ± 0.290	7.90 ± 0.137	0.16 ± 0.036	1.54 ± 0.038	0.21	1.50	247.45	23.48	5.60 ± 0.225	363 ± 1.487	−0.970 ± 0.006
945	54.08 ± 0.124	35.84 ± 0.096	8.21 ± 0.136	0.12 ± 0.018	1.72 ± 0.068	0.22	1.50	298.82	20.80	5.30 ± 0.032	366 ± 1.049	−0.941 ± 0.015

[a]Values are presented as mean ± SEM; *n* = 3.

Downloaded from https://journals.asm.org/journal/aem on 04 November 2026 by 2a02:2455:1ca1:2600:a7cd:7757:1758:28a8.

Additional details on the methods and data analysis are provided in Text S4 through S10, along with Data Set S1.

Data integration and statistical analysis

Principal component analysis (PCA) and partial least squares discriminant analysis (PLS-DA) were performed using SIMCA-P 9.0 (Umetrics AB, Sweden). Correlations between operational taxonomic units (OTUs) and FT-ICR MS data sets were evaluated according to the experimental design, with time as the sole explanatory factor and three biological replicates per sampling point. Data integration analyses were restricted to the 470-, 605-, and 945-day incubation samples because complete paired FT-ICR MS and 16S rRNA gene amplicon data sets were only available for these time points. An orthogonal partial least squares (OPLS) model was subsequently constructed to integrate FT-ICR MS and 16S rRNA gene amplicon data. Model validation was performed using leave-one-out cross-validation, retaining two predictive components. Variable importance was assessed based on each variable's contribution to the first predictive component. OPLS analyses were conducted using SIMCA-P version 13.0.1 (Umetrics AB, Sweden).

Prior to modeling, the data were scaled to unit variance. The OPLS model comprised one predictive component and five orthogonal components (1 + 5 + 0), accounting for 92.3% of the cumulative variation in the X matrix ($R^2X = 0.923$) and 100% of the variation in the response variable ($R^2Y = 1.000$). Model predictability was assessed by cross-validation, resulting in a cumulative Q^2 value of 0.940. Model robustness was further evaluated using permutation testing with 100 permutations.

RESULTS

Temporal changes in molecular-formula composition and sulfur-containing compounds during anaerobic incubation

The molecular formulas detected in the water phases of heavy-oil microcosms incubated with oil from the Pitch Lake, Trinidad and Tobago, were analyzed by FT-ICR MS, which provides ultrahigh mass accuracy and resolving power (4, 22, 25–28). Across all samples and experimental replicates over the 945-day incubation, 4,499 molecular formulas were assigned, with their distribution among the CHO, CHOS, CHON, and CHONS classes changing over time (Fig. 1 and 2; Fig. S1; Table S1). The first water-phase sample was collected on day 93 to allow water-soluble compounds to dissolve in the freshly added water phase and to equilibrate with the oil. Hence, day 93 was considered the starting point of the sampling period. The total number of assigned molecular formulas increased from 2,219 at day 93 to 3,607 at day 604, followed by a slight decrease to 3,589 at day 945 (Fig. 1; Table S1). CHO formulas increased from 785 at day 93 to 1,043 at day 604, followed by a slight decrease to 1,033 at day 945. In contrast, the number of CHOS formulas increased over the incubation period, from 1,176 to 2,151, with their relative contribution increasing from 53.0% to 59.9%. CHON formulas increased from 236 at day 93 to 418 at day 604 before decreasing to 310 at day 945, whereas the number of CHONS formulas generally increased over time, from 22 on day 93 to 97 on day 604, and remained relatively stable at 95 on day 945. Overall, the molecular-formula distribution shifted toward sulfur-containing classes, particularly CHOS.

UpSet analysis showed that 1,836 formulas were shared across all five incubation periods, whereas 379 and 290 formulas were unique to days 604 and 945, respectively (Fig. S2). Changes in molecular formulas were also evident in the van Krevelen plots, mass-edited H/C and O/C ratio distributions (Fig. 1A, B and 2; Fig. S1). Furthermore, the number of unique CHOS formulas increased 25-fold between days 93 and 945 (Fig. S3), accompanied by increasing compositional diversity of the CHOS molecular-formula pool (Fig. 2; Table S1). $CHOS_1$ formulas remained the dominant sulfur-containing subclass throughout the incubation, whereas $CHOS_2$, $CHOS_3$, and $CHOS_4$ generally increased with incubation time (Fig. 2, inset rings). A subset of CHOS formulas was detected at all sampling times and occupied a relatively consistent region of van Krevelen space (Fig. S4). Their relative inter-sample ranking among samples varied over time, indicating

Downloaded from https://journals.asm.org/journal/aem on 04 November 2026 by 2a02:2455:1ca1:2600:a7cd:7757:1758:28a8.

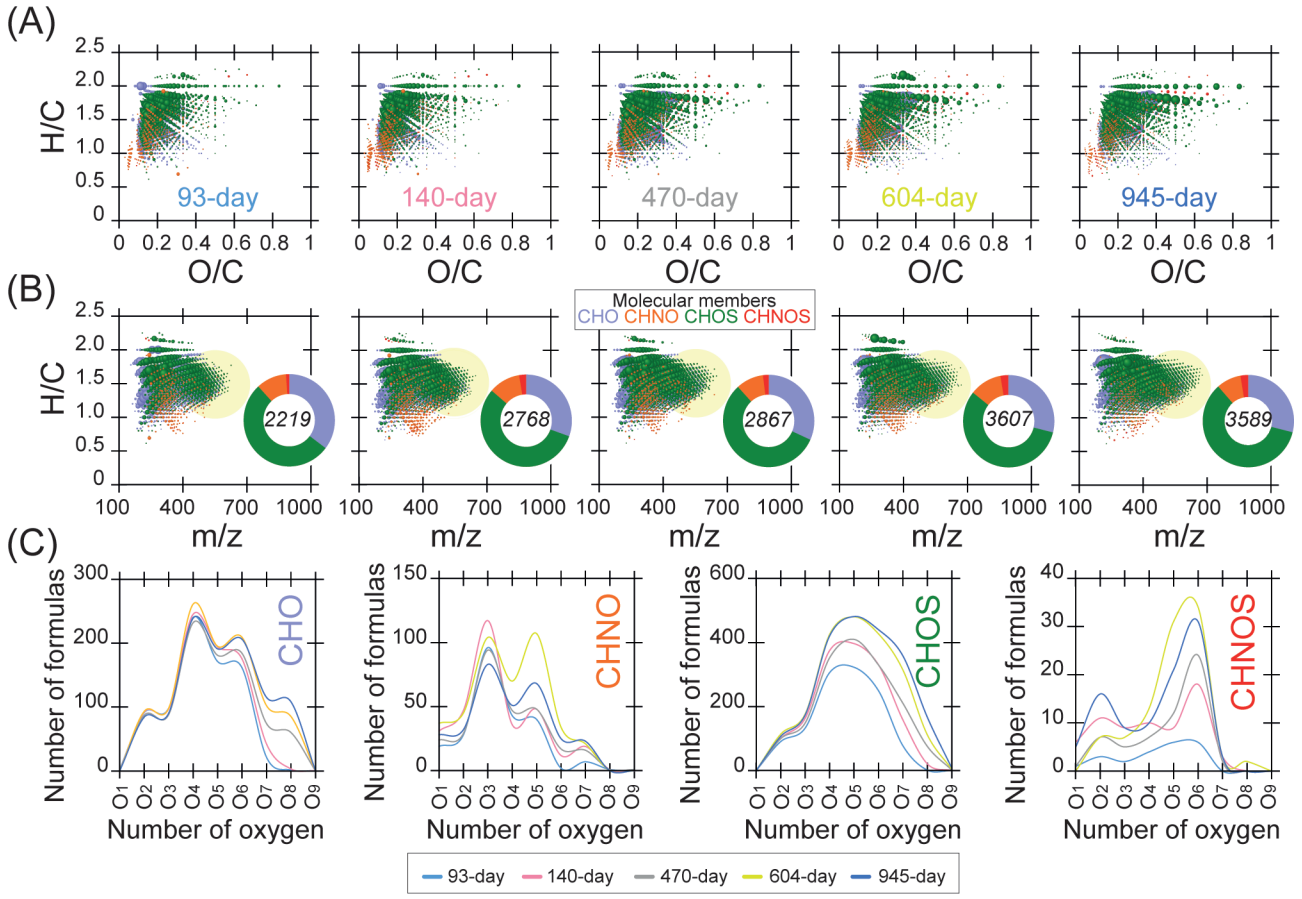

FIG 1 Distributional changes of oil molecular formulas over 945 days in the water phases of microcosm incubations with heavy oil from the Pitch Lake, Trinidad and Tobago, as determined by negative electrospray ionization 12T FT-ICR MS. (A and B) van Krevelen diagrams and mass-edited H/C ratios. Bubbles indicate individual oil molecular formulas, with bubble sizes corresponding to the average mass peak intensities. Molecular formulas in the water phase are classified as CHO (blue), CHNO (orange), CHOS (green), and CHNOS (red). The number inside each ring in panel B indicates the total number of formulas detected at each incubation time. The pale-yellow circle highlights the extension of the molecular formula distribution toward higher molecular weights. (C) Temporal changes in the number of oxygen atoms incorporated into the different molecular formulas.

changes in their relative representation. Because this analysis includes only formulas detected at every time point, it represents the shared CHOS pool and excludes formulas that appeared or disappeared during incubation. The shared formulas remained concentrated in the low-O/C region of van Krevelen space (Fig. S4).

The intensity-weighted elemental formulas also changed over the incubation (Table 1). Hydrogen and carbon showed an overall decrease during the incubation, from 54.76 to 54.08 atom% and from 36.68 to 35.84 atom%, respectively. Hydrogen decreased gradually, with a slight increase at 604 days, whereas carbon showed a slight increase at 140 days before declining thereafter. In contrast, oxygen increased overall, from 7.19 to 8.21 atom%, with a slight decrease at 140 days and a small decrease at 604 days. Nitrogen increased from 0.17 to 0.26 atom% at 140 days, followed by a gradual decline to 0.12 atom% at 945 days. Sulfur showed a consistent increase throughout the incubation, from 1.18 to 1.72 atom%. The O/C ratio increased from 0.19 to 0.22, whereas the C/S ratio decreased from 31.21 to 20.80. An increase in oxygen-containing molecular series within the O_4–O_6 classes was also observed (Fig. 1C). DBE varied only slightly across the incubation, ranging from 5.3 to 5.9. The intensity-weighted mean *m/z* increased overall from 344 at day 93 to 366 at day 945, despite intermediate fluctuations, corresponding to a 6.4% increase. Over the same period, intensity-weighted carbon oxidation state (Zc) increased from −1.048 to −0.941 (Table 1).

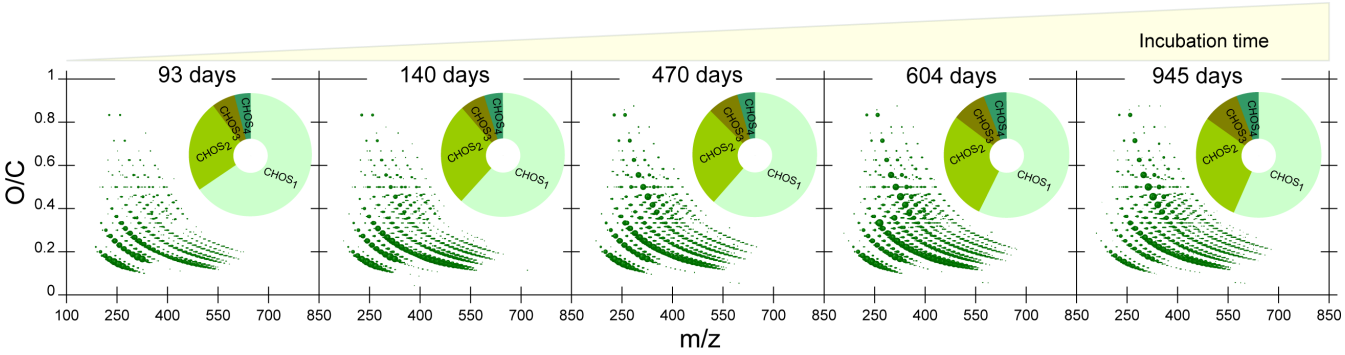

FIG 2 Distributional changes in the mass-edited O/C ratios of CHOS molecular formulas over 945 days in the water phases of microcosm incubations with heavy oil from the Pitch Lake, Trinidad and Tobago, as determined by negative electrospray ionization 12T FT-ICR MS. Bubbles represent individual CHOS molecular formulas, with bubble size corresponding to the average mass-peak intensity. Inset rings indicate molecular formula classes: $CHOS_1$ (light green), $CHOS_2$ (yellow-green), $CHOS_3$ (olive), and $CHOS_4$ (teal green). Mass-edited O/C ratio plots for CHO, CHNO, and CHNOS are provided in Fig. S1.

Time-dependent clustering and molecular evolution of heavy oil water-phase compositions

We further evaluated the FT-ICR MS data of water phases using principal component analysis (Fig. 3A) and partial least squares discriminant analysis (Fig. 3B), which revealed clear separation according to incubation time. The PCA distinguished early samples (Group 1: 93-, 140-, and 470-day incubations) from later stages (Group 2: 604 days and Group 3: 945 days), with the first two principal components explaining 63.6% of the variance, while the PLS-DA model [R^2X(cum) = 63.2%, R^2Y(cum) = 37.3%, Q^2(cum) = 90%] further supported this separation, resolving three temporally distinct groups with different molecular profiles. Consistent with these temporal groupings, the distribution of discriminant molecular formulas among the major molecular classes (CHO, CHNO, CHOS, and CHNOS) also varied across the three groups (Fig. 3C through H). CHO and CHNO formulas increased from Group 1 to Group 2 and subsequently decreased in Group 3, whereas CHOS formulas increased progressively across the groups, with the greatest representation in Group 3 (Table S2). In contrast, the CHNOS class remained comparatively stable across the three groups (Table S2). These patterns indicate that the temporal separation observed in the multivariate analyses was associated with systematic shifts in molecular formulas, particularly the progressive enrichment of CHOS-class formulas during incubation.

Correspondingly, distinct temporal trends in molecular unsaturation, as reflected by the DBE distribution (Fig. S5), were observed among the molecular classes. Molecular formulas were classified as having low (DBE <4), moderate (4 ≤ DBE ≤ 7), or high (DBE >7) degrees of unsaturation (29). CHO-class formulas exhibited a pronounced increase in moderately (4 ≤ DBE ≤ 7) and highly unsaturated (DBE >7) formulas from Group 1 to Group 2, followed by substantial decreases in Group 3. CHNO-class formulas showed a similar pattern, although the increase in moderately unsaturated formulas was less pronounced, with both moderately and highly unsaturated formulas increasing from Group 1 to Group 2 and subsequently declining in Group 3. In contrast, CHOS-class formulas exhibited a distinct temporal pattern, with low-DBE formulas (DBE <4) increasing progressively across the incubation groups. Moderately unsaturated formulas also increased substantially across the groups, whereas highly unsaturated formulas increased from Group 1 to Group 2 before declining in Group 3. CHNOS-class formulas displayed comparatively minor changes in their DBE distribution across the three groups.

Overall, these results indicate class-dependent temporal reorganization of molecular unsaturation during anaerobic incubation. CHO and CHNO formulas were characterized by enrichment of moderately and highly unsaturated compounds at the intermediate incubation stage, whereas CHOS formulas showed progressive accumulation of low- and moderately unsaturated compounds and a decline in highly unsaturated formulas at the

Downloaded from https://journals.asm.org/journal/aem on 04 November 2026 by 2a02:2455:1ca1:2600:a7cd:7757:1758:28a8.

Downloaded from https://journals.asm.org/journal/aem on 04 November 2026 by 2a02:2455:1ca1:2600:a7cd:7757:1758:28a8.

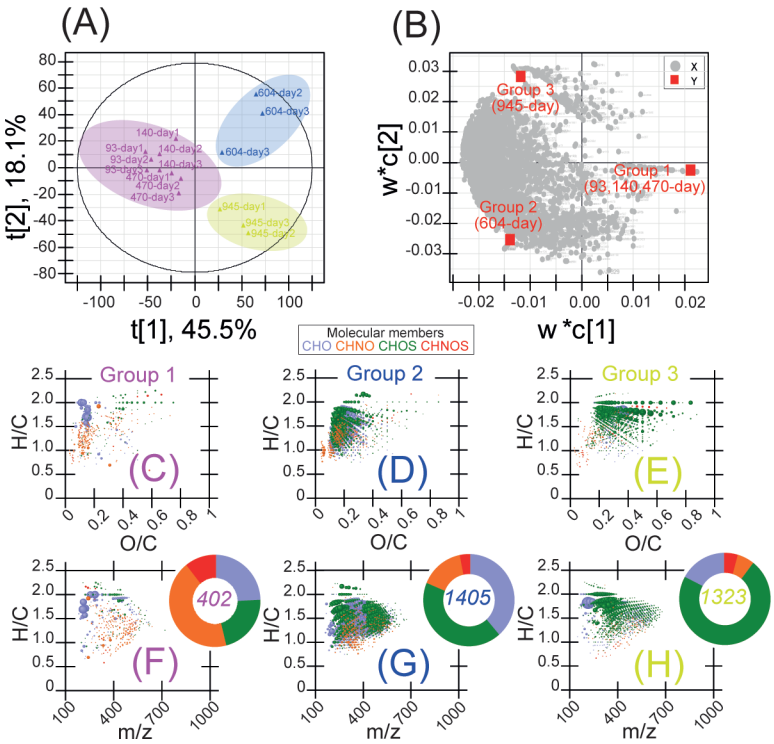

FIG 3 Negative electrospray ionization 12T FT-ICR mass spectrometry data of the water phases collected after 93, 140, 470, 604, and 945 days from triplicate incubations with heavy oil from the Pitch Lake, Trinidad and Tobago. (A) PCA and (B) PLS-DA w*c[1]/w*c[2] loading scatter plots of the FT-ICR MS data from the oil-water phases over 945 days of incubation, with the three main classes represented by red squares. X represents the data matrix with scaled intensities for each *m/z* and sample, and Y represents the dummy response variable of the groups. Panels C, D, and E show van Krevelen plots (top panels), while panels F, G, and H display H/C ratio versus mass-to-charge (*m/z*) plots (bottom panels) for the discriminant masses in each group. Group 1 represents the discriminant masses corresponding to the 93-, 140-, and 470-day incubations, while Groups 2 and 3 correspond to the discriminant masses from the 604- and 945-day incubations, respectively. Bubbles indicate individual molecular formulas, with bubble sizes corresponding to the average mass peak intensities. Molecular formulas in the water phase are classified as CHO (purple), CHNO (orange), CHOS (green), and CHNOS (red). The number in each ring indicates the total number of molecular formulas extracted for each group. Additional information on the degree of unsaturation of these three groups is provided in Fig. S5.

later stage. In contrast, the DBE distribution of CHNOS formulas remained comparatively stable throughout incubation, with only modest changes in the relative abundance of the three unsaturation classes.

Time-dependent association of microbial community shifts and chemical formula changes

OPLS analysis integrating microbial data and FT-ICR MS-derived molecular profiles revealed clear temporal separation across 470-, 604-, and 945-day incubations (Fig. 4A and B), indicating coordinated shifts in microbial composition and water-phase molecular formulas. Over time, microbial community composition changed substantially, as indicated by the microbial taxonomic patterns in Fig. 4B, whereas the number of discriminant molecular masses (*m/z*) increased (Fig. 4C through E), indicating changes in community composition alongside increasing molecular complexity (30). In parallel, microbial communities showed temporal shifts in the occurrence of taxa, with *Desulfobacterales*, *Desulfovibrio*, and *Defluviitoga* detected at different sampling stages, including the later stages (Fig. 4B; Table S3). CHOS-class formulas were low at the early

Downloaded from https://journals.asm.org/journal/aem on 04 November 2026 by 2a02:2455:1ca1:2600:a7cd:7757:1758:28a8.

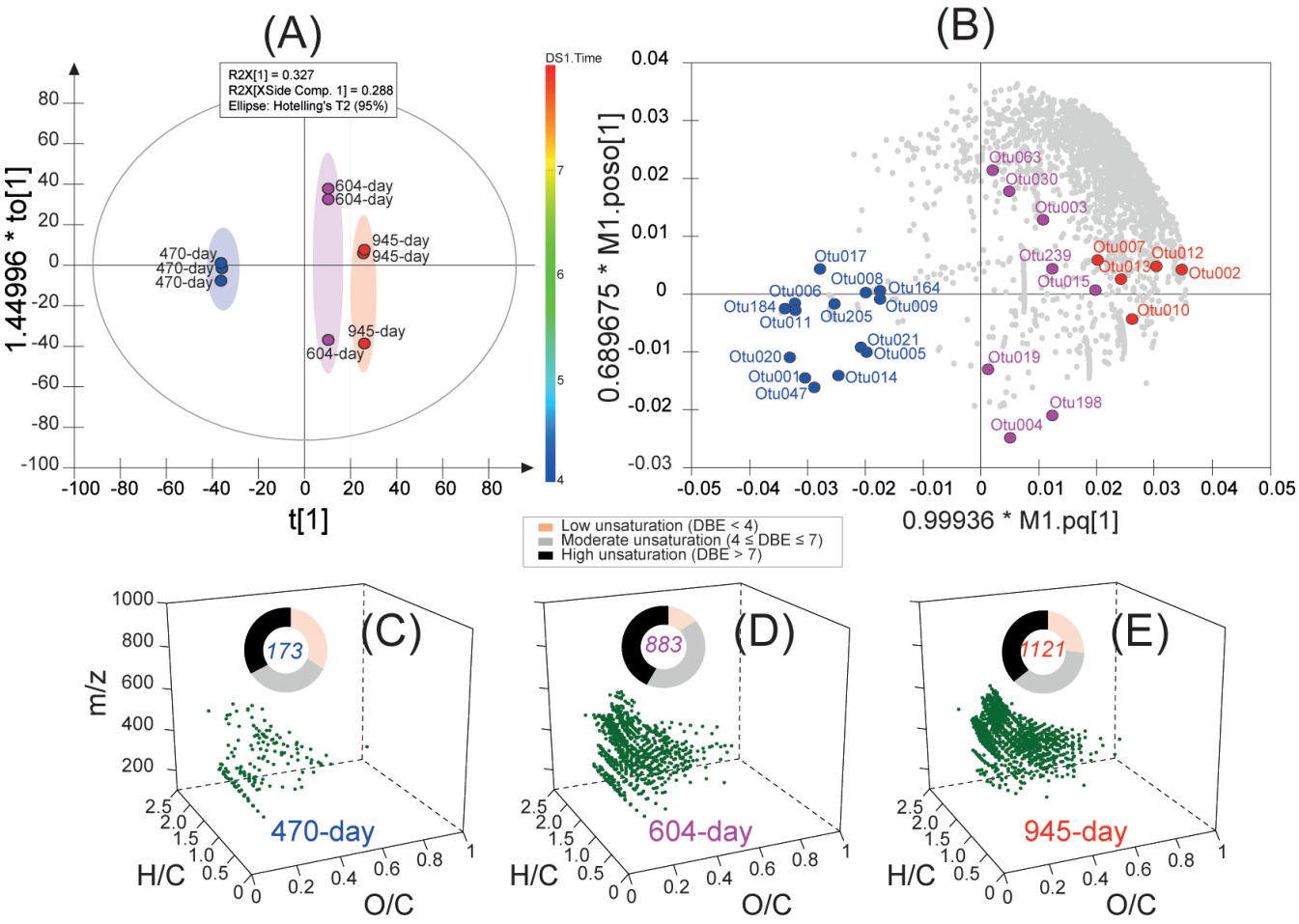

FIG 4 OPLS score plot (A) and OPLS loading plot (B) of the water phase extracts collected after 470, 604, and 945 days of incubation. Panels C, D, and E show 3D visualizations of the most correlated *m/z* signals, based on their variable contribution to the first component of the OPLS model, illustrating the chemical space of molecular formulas in relation to the most abundant OTUs during the incubation period. The most correlated formulas primarily correspond to CHOS molecular formulas. The corresponding OTU IDs are listed in Table S3. The inset rings represent the number of correlated formulas. Ring color indicates the number of formulas with low (DBE < 4; peach), moderate (4 ≤ DBE ≤ 7; light gray), and high (DBE > 7; black) degrees of unsaturation, respectively.

incubation but increased noticeably at 604 and 945 days (Fig. 4C through E; Table S3), consistent with the presence of sulfate-associated taxa such as *Desulfovibrio*, *Mesotoga*, and *Defluviitoga*.

Simultaneously, molecular formulas with low degrees of unsaturation (DBE <4) increased clearly with prolonged incubation, from 59 formulas at 470 days to 306 formulas at 945 days (Table S4). Molecular formulas with moderate (4 ≤ DBE ≤ 7) and high (DBE >7) degrees of unsaturation also increased substantially, reaching 416 and 399 formulas, respectively, at 945 days (Table S4). Overall, these patterns indicate a progressive enrichment of highly unsaturated molecular formulas during prolonged incubation, consistent with a shift toward greater molecular unsaturation over time.

Temporal patterns in CHOS-class formulas associated with microbial community changes

We also examined the associations between specific microbial genera and $CHSO_2$, $CHSO_3$, and $CHSO_4$ molecular formulas at 470, 604, and 945 days of incubation (Fig. 5; Table S5). Distinct temporal patterns were observed in the degree of unsaturation of molecular formulas associated with different microbial genera. $CHSO_2$ molecular formulas showed an overall decline by day 945. Low- and moderately unsaturated formulas

Downloaded from https://journals.asm.org/journal/aem on 04 November 2026 by 2a02:2455:1ca1:2600:a7cd:7757:1758:28a8.

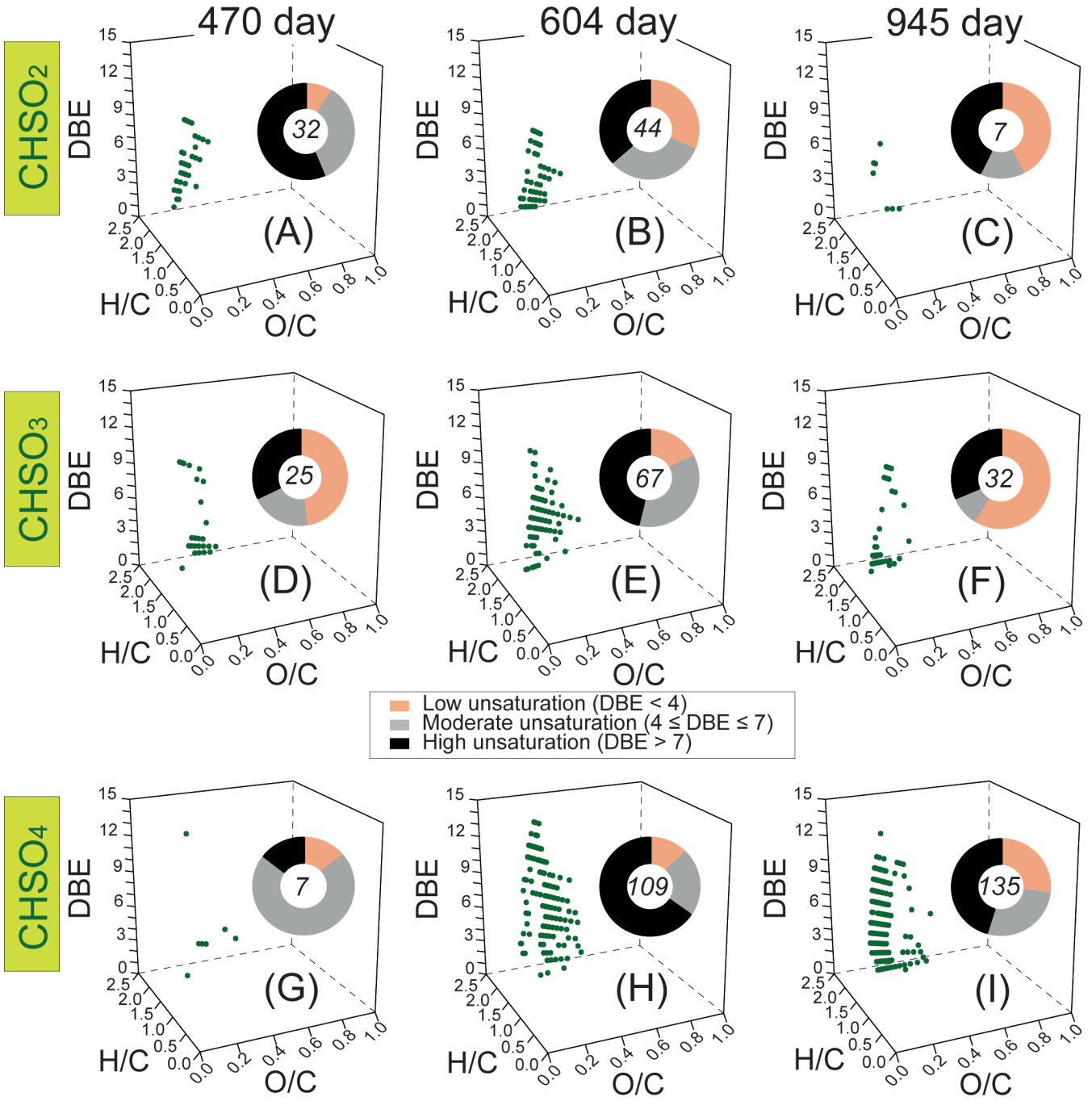

FIG 5 3D visualizations of $CHSO_2$ (A–C), $CHSO_3$ (D–F), and $CHSO_4$ (G–I) class formulas after 470 (A, D, G), 604 (B, E, H), and 945 days (C, F, I) of incubation. The molecular formulas shown were extracted from the CHOS molecular formula pool presented in Fig. 4C through E. Dots along the same lines represent molecular formulas with the same DBE. The inset rings indicate the number of correlated molecular formulas. Ring colors represent the proportions of formulas with low (DBE <4; peach), moderate (4 ≤ DBE ≤ 7; light gray), and high (DBE >7; black) degrees of unsaturation.

increased slightly from day 470 to day 604, from 3 to 14 and from 11 to 14 formulas, respectively, whereas highly unsaturated formulas decreased from 18 to 16. By day 945, all three unsaturation classes had declined substantially, with only three low-, one moderately, and three highly unsaturated formulas remaining (Fig. 5A through C; Table S5). $CHSO_3$ molecular formulas showed a distinct temporal pattern, with low-DBE formulas remaining stable between days 470 and 604 before increasing at day 945. In contrast, moderately and highly unsaturated formulas increased markedly from day

Downloaded from https://journals.asm.org/journal/aem on 04 November 2026 by 2a02:2455:1ca1:2600:a7cd:7757:1758:28a8.

470 to day 604, from 5 to 24 and from 8 to 31 formulas, respectively, followed by substantial declines at day 945 (Fig. 5D through F; Table S5). $CHSO_4$ molecular formulas increased substantially throughout the incubation period, with low-DBE formulas increasing progressively from 1 to 14 and then 37 formulas, while moderately and highly unsaturated formulas increased markedly by day 604 and remained elevated at day 945. In particular, highly unsaturated $CHSO_4$ formulas increased from 1 formula at day 470 to 71 at day 604 and slightly decreased at day 945, with 61 formulas (Fig. 5G through I; Table S5). These temporal patterns were associated with shifts in sulfur-related microbial genera, including *Desulfovibrio*, *Mesotoga*, and *Defluviitoga*. Overall, the results indicate that changes in microbial community composition were accompanied by shifts in the distribution and degree of unsaturation of associated $CHSO_{2\leq n\leq 4}$ molecular classes, particularly the pronounced increase in $CHSO_4$ molecular formulas during prolonged incubation.

DISCUSSION

Selective enrichment of CHOS-class formulas and sulfur transformation processes during incubation

FT-ICR MS analysis of water phases extracted from incubated heavy oil samples revealed a highly complex chemical diversity dominated by heteroatom-containing compounds, including CHO-, CHOS-, CHNO-, and CHNOS-class formulas. Among these, CHOS formulas exhibited a pronounced and persistent increase over the incubation period, exceeding the relative changes observed in other compound classes. This selective enrichment is consistent with systematic changes in sulfur-containing molecular formulas during incubation.

The first water-phase sample was collected on day 93 to allow water-soluble compounds to dissolve in the freshly added water phase and to equilibrate with the oil for 3 months. Hence, day 93 has to be considered as the starting point of the monitoring. Thus, the molecular formulas observed at the first sampling point may reflect both rapid abiotic release of compounds already present in the oil and early microbial activity. Some CHOS and CHO compounds may therefore represent pre-existing oil constituents transferred into the water phase rather than compounds newly formed during incubation. In addition, killed-control microcosms were not included in the experimental design, and therefore, the relative contributions of microbial and abiotic processes to the observed molecular changes cannot be directly resolved.

As reported previously (4), physical extraction of the oil using ultra-pure water showed a fractionation of functionalized compounds into the water phase, providing a reference for the molecular compounds released in the absence of microbial activity. The molecular formulas observed by FT-ICR MS, however, differed from those of the ultra-pure water extract, which is consistent with a potential microbial contribution to the water-phase molecular formulas. This enrichment may reflect a combination of microbial transformation and sulfur incorporation, as well as differential partitioning and persistence of sulfur-containing compounds in the water phase. Because sulfur-containing compounds are not inherently more water-soluble than non-sulfur-containing compounds, the observed increase in CHOS formulas cannot be attributed to solubility alone. Thus, the increase in CHOS formulas reflects changes in the molecular formulas of the water phase and may result from multiple processes, including microbial transformation, sulfur incorporation, and differential partitioning or persistence. These observations are consistent with progressive transformation processes under anaerobic conditions and with a potential association with microbial sulfur-cycling in hydrocarbon-rich environments, as previously reported in sulfate-amended, hydrocarbon-impacted sediments where sulfate availability alters microbial competition and community structure (26).

Accordingly, the strong temporal increase in CHOS-class formulas, together with their oxidized character, suggests an association with ongoing transformation of oil-derived substrates rather than reflecting only residual constituents of the parent oil (4).

Downloaded from https://journals.asm.org/journal/aem on 04 November 2026 by 2a02:2455:1ca1:2600:a7cd:7757:1758:28a8.

Nevertheless, continued dissolution of pre-existing oil-derived compounds may also contribute to the observed temporal pattern. In anoxic systems, CHOS formation can result from both microbial sulfur transformation and abiotic reactions involving reduced sulfur species, making it difficult to fully separate these contributions. However, microbial sulfate reduction and sulfide-mediated transformations are commonly implicated in the formation of organosulfur compounds under such conditions (4, 26). Similar molecular signatures reported from Pitch Lake environments have likewise been associated with active microbial transformation processes (4). Overall, the observed CHOS accumulation is consistent with sulfur transformation processes potentially involving both microbial activity and secondary chemical reactions but does not by itself establish a direct microbial cause or distinguish the relative contributions of these processes.

Abiotic sulfurization versus microbial co-metabolism driving CHOS formation

To investigate the potential origins of CHOS compounds, we considered two possible pathways: (i) abiotic sulfurization and (ii) microbial co-metabolism. Abiotic sulfurization involves the incorporation of sulfur or hydrogen sulfide into unsaturated organic compounds under anoxic conditions, forming thiols, monosulfides, and disulfides through non-biological reactions (12). In the microcosms, microbial sulfate reduction may have contributed to hydrogen sulfide production, which could provide conditions conducive to such reactions. However, the observed CHOS molecular formulas are dominated by highly oxygenated species, including formulas consistent with SO_3- and SO_4-like moieties, suggesting that abiotic sulfurization alone may not fully explain their formation and that microbial co-metabolism must also contribute. Nevertheless, molecular formula assignments alone cannot unambiguously distinguish between these pathways. Stable isotope measurements were not performed in this study and therefore cannot be used to further differentiate their contributions. Accordingly, both abiotic sulfurization and microbial co-metabolism are considered potential pathways for CHOS formation rather than definitive mechanistic assignments.

An alternative and potentially more consistent explanation is microbial co-metabolism, in which sulfur-containing compounds may be transformed indirectly by broad-specificity enzymes during the degradation of more readily utilizable substrates such as CHO-, CHNO-, or CHNOS-class formulas. In this process, transformation occurs without direct energy or carbon gain from the affected compounds. Co-metabolic transformations have been demonstrated in the sulfate-reducing, naphthalene-degrading culture N47, where a range of aromatic and heterocyclic compounds were transformed during growth on primary substrates (31, 32). These reactions have been attributed to enzymatic activity with broad substrate specificity at the early stages of degradation, leading to the formation of partially transformed products that may persist when subsequent metabolic pathways are limited. In our system, the observed correlations between specific microbial taxa and CHOS-class formulas, particularly $CHSO_2$, $CHSO_3$, and $CHSO_4$, are consistent with an association between microbial community composition and the distribution of sulfur-containing compounds. However, these correlations do not by themselves establish a causal relationship between specific microbial taxa and CHOS transformations. CHOS compounds exhibited pronounced temporal changes, consistent with their reactive behavior under anoxic, biologically active conditions. Similar enrichment patterns of heterocyclic compounds have been reported in contaminated aquifers and attributed to co-metabolic transformation processes (33). These observations are consistent with a contribution of microbial co-metabolism to the observed CHOS diversity in the microcosms, potentially in conjunction with secondary abiotic reactions via microbially produced sulfide. However, the absence of killed-control microcosms, where potential chemical reactants like sulfide have been added, prevents quantitative differentiation of microbial and abiotic contributions in this case.

Downloaded from https://journals.asm.org/journal/aem on 04 November 2026 by 2a02:2455:1ca1:2600:a7cd:7757:1758:28a8.

CHOS accumulation and its role in hydrocarbon degradation under anoxic conditions

CHOS-containing compounds may accumulate because they are less readily transformed by microbial communities compared to hydrocarbons. These compounds may represent partially transformed products resulting from incomplete or inefficient microbial processing rather than terminal degradation end-products. Microbial co-metabolism may contribute to this accumulation, as heterocyclic compounds can undergo transformation without necessarily serving as growth substrates for the microorganisms involved (32). Alternatively, some CHOS compounds may persist because they are less susceptible to anaerobic microbial degradation or because microorganisms capable of using them as growth substrates are absent or present at low abundance. Previous studies have shown that sulfur-containing heterocyclic compounds can be less susceptible to anaerobic biodegradation than nitrogen- and oxygen-containing heterocycles, although susceptibility varies among individual compounds and environmental conditions (32–34).

However, the molecular distribution of CHOS molecular formulas detected by negative-mode electrospray ionization FT-ICR MS may be influenced by differences in ionization and detection efficiencies among sulfur-containing compound classes, which can affect their relative abundances. Reduced sulfur compounds, such as thiols and sulfides, may be underrepresented under the applied analytical conditions. Thus, the predominance of oxidized CHOS species does not necessarily indicate the absence of reduced abiotic sulfurization products. Consequently, the CHOS molecular distribution alone cannot fully resolve the relative contributions of biotic and abiotic sulfurization pathways.

Environmental factors such as high temperature, salinity, and elevated hydrocarbon concentrations may further constrain microbial activity and diversity, potentially limiting the capacity for complete degradation. The structural complexity of crude oil requires diverse microbial communities to process the wide range of O-, N-, and S-functionalized molecular formulas. Limited microbial richness, metabolic specialization, and cross-feeding interactions may therefore restrict the further transformation or utilization of some CHOS-containing molecular formulas. Studies of microbial degradation of complex organic substrates, including polymeric hydrocarbons, further demonstrate that microbial transformation can be incomplete and strongly dependent on the physiological capabilities of individual organisms (35). Consequently, the accumulation of CHOS-, CHO-, CHNO-, and CHNOS-class formulas may reflect constrained microbial transformation and/or limited utilization under energy-limited, anoxic conditions. However, the present FT-ICR MS data cannot distinguish between incomplete co-metabolic transformation and limited utilization of CHOS compounds by organisms that might be able to fully degrade such compounds but are limited by environmental factors, leading to partial degradation.

Microbial diversity and implications for hydrocarbon transformation in oil reservoirs

The vast chemical diversity of oil, which includes thousands of distinct molecular signatures (36, 37), contrasts with the comparatively low microbial alpha diversity observed in oil reservoirs. Reported values range from 91 to 319 OTUs in Pitch Lake oil droplets and up to 558 OTUs in water droplets from U.S. heavy oil reservoirs, with Shannon indices typically between 1.5 and 5 (3, 38, 39). These observations indicate that microbial diversity in oil systems is relatively limited and strongly influenced by environmental constraints, including water availability. Moreover, only a subset of these microorganisms is capable of hydrocarbon degradation, while many are non-degraders or methanogens that depend on fermentation products such as hydrogen and short-chain fatty acids (40, 41). Although recent studies have expanded the range of known metabolic capabilities, including methanogenic oxidation of methoxylated aromatics

Downloaded from https://journals.asm.org/journal/aem on 04 November 2026 by 2a02:2455:1ca1:2600:a7cd:7757:1758:28a8.

and long-chain alkanes (42, 43), the proportion of actively degrading taxa remains small relative to the chemical complexity of oil.

This difference raises questions regarding how a limited set of microbial metabolisms can contribute to the transformation of such chemically diverse mixtures. Given that many model organisms, such as *Escherichia coli*, utilize only a restricted range of substrates (44) and that even specialized hydrocarbon-degrading cultures such as strain N47 act on relatively narrow compound sets (45, 46), microbial diversity alone may not fully account for the breadth of observed chemical transformations in oil reservoirs. These considerations are consistent with the potential importance of co-metabolic processes in enabling broader transformation of complex oil-derived compounds. Nevertheless, the present data support an association between microbial community dynamics and CHOS molecular changes rather than demonstrating that microbial co-metabolism is responsible for the observed transformations.

Conclusion

Long-term anaerobic incubation of heavy oil in controlled microcosms resulted in pronounced and systematic changes in both chemical formulas and microbial community structure. Ultrahigh-resolution FT-ICR MS analysis revealed a highly diverse molecular pool dominated by CHO-, CHOS-, CHNO-, and CHNOS-class formulas, with CHOS molecular formulas showing the most pronounced and continuous increase over time. These changes were accompanied by shifts in hydrocarbon-related molecular classes and progressive enrichment of oxygen- and sulfur-containing molecular formulas. In parallel, microbial communities exhibited reduced diversity and increased relative abundance of taxa associated with anaerobic and sulfur-related metabolisms, including *Desulfovibrio*, *Desulfobacterales*, and *Defluviitoga*. Multivariate analyses further demonstrated coordinated temporal relationships between microbial composition and molecular profiles. These findings indicate that even low-diversity microbial communities can induce substantial and systematic transformation of heavy oil under anaerobic conditions, leading to the reorganization of heteroatom-rich molecular pools. The results highlight the importance of microbial activity, particularly processes linked to sulfur-cycling, in shaping the molecular evolution of oil in subsurface-like environments.

ACKNOWLEDGMENTS

This work was supported by the EU-Horizon 2020 program, ERC-advanced grant EcOILogy (grant number 666952) to R.U. Meckenstock, and by the German Research Foundation (DFG) project BR 5493/1–1 to V. Brauer.

AUTHOR AFFILIATIONS

[1]Research Unit Analytical BioGeoChemistry, Helmholtz Munich, Neuherberg, Germany
[2]Chair of Analytical Food Chemistry, Technical University of Munich, Freising, Germany
[3]Environmental Microbiology and Biotechnology, Aquatic Microbiology, University of Duisburg-Essen, Essen, Germany

PRESENT ADDRESS

Mark Pannekens, IWW Zentrum Wasser, Mülheim an der Ruhr, Germany

AUTHOR ORCIDs

Mourad Harir http://orcid.org/0000-0003-3758-2713
Lisa Voskuhl http://orcid.org/0000-0001-5776-5491
Rainer U. Meckenstock http://orcid.org/0000-0001-7786-9546

Downloaded from https://journals.asm.org/journal/aem on 04 November 2026 by 2a02:2455:1ca1:2600:a7cd:7757:1758:28a8.

FUNDING

Funder	Grant(s)	Author(s)
Horizon	2020 program	Rainer U. Meckenstock
ERC-advanced	666952	Rainer U. Meckenstock
German Research Foundation	BR 5493/1-1	Verena Brauer

AUTHOR CONTRIBUTIONS

Mark Pannekens, Data curation, Investigation, Methodology, Validation | Lisa Voskuhl, Methodology, Resources, Validation | Verena Brauer, Methodology, Resources, Validation | Rainer U. Meckenstock, Conceptualization, Resources, Validation.

ADDITIONAL FILES

The following material is available online.

Supplemental Material

Data Set S1 (AEM01253-26-S0001.xlsx). FT-ICR MS data.
Supplemental material (AEM01253-26-S0002.pdf). Text S1 to S10, Fig. S1 to S5, and Tables S1 to S5.

REFERENCES

1. Magot M, Ollivier B, Patel BK. 2000. Microbiology of petroleum reservoirs. Antonie Van Leeuwenhoek 77:103–116. https://doi.org/10.1023/a:1002434330514
2. Head IM, Jones DM, Larter SR. 2003. Biological activity in the deep subsurface and the origin of heavy oil. Nature 426:344–352. https://doi.org/10.1038/nature02134
3. Pannekens M, Voskuhl L, Meier A, Müller H, Haque S, Frösler J, Brauer VS, Meckenstock RU. 2020. Densely populated water droplets in heavy-oil seeps. Appl Environ Microbiol 86:11. https://doi.org/10.1128/AEM.00164-20
4. Meckenstock RU, von Netzer F, Stumpp C, Lueders T, Himmelberg AM, Hertkorn N, Schmitt-Kopplin P, Harir M, Hosein R, Haque S, Schulze-Makuch D. 2014. Oil biodegradation. Water droplets in oil are microhabitats for microbial life. Science 345:673–676. https://doi.org/10.1126/science.1252215
5. Pannekens M, Kroll L, Müller H, Mbow FT, Meckenstock RU. 2019. Oil reservoirs, an exceptional habitat for microorganisms. N Biotechnol 49:1–9. https://doi.org/10.1016/j.nbt.2018.11.006
6. Pannekens M, Voskuhl L, Mohammadian S, Köster D, Meier A, Köhne JM, Kulbatzki M, Akbari A, Haque S, Meckenstock RU. 2021. Microbial degradation rates of natural bitumen. Environ Sci Technol 55:8700–8708. https://doi.org/10.1021/acs.est.1c00596
7. Beilig S, Pannekens M, Voskuhl L, Meckenstock RU. 2024. Assessing anaerobic microbial degradation rates of crude light oil with reverse stable isotope labelling and community analysis. Front Microbiomes 3:1324967. https://doi.org/10.3389/frmbi.2024.1324967
8. Brassell SC, Lewis CA, de Leeuw JW, de Lange F, Damsté JSS. 1986. Isoprenoid thiophenes: novel products of sediment diagenesis? Nature 320:160–162. https://doi.org/10.1038/320160a0
9. Cyr TD, Payzant JD, Montgomery DS, Strausz OP. 1986. A homologous series of novel hopane sulfides in petroleum. Org Geochem 9:139–143. https://doi.org/10.1016/0146-6380(86)90104-X
10. Schmid JC, Connan J, Albrecht P. 1987. Occurrence and geochemical significance of long-chain dialkylthiacyclopentanes. Nature 329:54–56. https://doi.org/10.1038/329054a0
11. Sinninghe Damst'e JS, Rijpstra WIC, Kock-van Dalen AC, De Leeuw JW, Schenck PA. 1989. Quenching of labile functionalised lipids by inorganic sulphur species: evidence for the formation of sedimentary organic sulphur compounds at the early stages of diagenesis. Geochim Cosmochim Acta 53:1343–1355. https://doi.org/10.1016/0016-7037(89)90067-7
12. Vairavamurthy A, Mopper K. 1987. Geochemical formation of organosulphur compounds (thiols) by addition of H_2S to sedimentary organic matter. Nature 329:623–625. https://doi.org/10.1038/329623a0
13. Werne JP, Hollander DJ, Behrens A, Schaeffer P, Albrecht P, Sinninghe Damsté JS. 2000. Timing of early diagenetic sulfurization of organic matter: a precursor-product relationship in Holocene sediments of the anoxic Cariaco Basin, Venezuela. Geochim Cosmochim Acta 64:1741–1751. https://doi.org/10.1016/S0016-7037(99)00366-X
14. Amrani A, Aizenshtat Z. 2004. Mechanisms of sulfur introduction chemically controlled: $\delta^{34}S$ imprint. Org Geochem 35:1319–1336. https://doi.org/10.1016/j.orggeochem.2004.06.019
15. Adam P, Philippe E, Albrecht P. 1998. Photochemical sulfurization of sedimentary organic matter: a widespread process occurring at early diagenesis in natural environments? Geochim Cosmochim Acta 62:265–271. https://doi.org/10.1016/S0016-7037(97)00332-3
16. Heitmann T, Blodau C. 2006. Oxidation and incorporation of hydrogen sulfide by dissolved organic matter. Chem Geol 235:12–20. https://doi.org/10.1016/j.chemgeo.2006.05.011
17. Lückge A, Horsfield B, Littke R, Scheeder G. 2002. Organic matter preservation and sulfur uptake in sediments from the continental margin off Pakistan. Org Geochem 33:477–488. https://doi.org/10.1016/S0146-6380(01)00171-1
18. Pohlabeln AM, Gomez-Saez GV, Noriega-Ortega BE, Dittmar T. 2017. Experimental evidence for abiotic sulfurization of marine dissolved organic matter. Front Mar Sci 4:364. https://doi.org/10.3389/fmars.2017.00364
19. Kohnen MEL, Sinninghe Damsté JS, Ten Haven HL, kock.-Van Dalen AC, Schouten S, De Leeuw JW. 1991. Identification and geochemical significance of cyclic di-and trisulphides with linear and acyclic isoprenoid carbon skeletons in immature sediments. Geochim Cosmochim Acta 55:3685–3695. https://doi.org/10.1016/0016-7037(91)90067-F
20. Westlake HE. 1946. The sulfurization of unsaturated compounds. Chem Rev 39:219–239. https://doi.org/10.1021/cr60123a002
21. Abdulla HA, Burdige DJ, Komada T. 2020. Abiotic formation of dissolved organic sulfur in anoxic sediments of Santa Barbara Basin. Org Geochem 139:103879. https://doi.org/10.1016/j.orggeochem.2019.05.009
22. Schulze-Makuch D, Haque S, Beckles D, Schmitt-Kopplin P, Harir M, Schneider B, Stumpp C, Wagner D. 2020. A chemical and microbial characterization of selected mud volcanoes in Trinidad reveals pathogens introduced by surface water and rain water. Sci Total Environ 707:136087. https://doi.org/10.1016/j.scitotenv.2019.136087

Downloaded from https://journals.asm.org/journal/aem on 04 November 2026 by 2a02:2455:1ca1:2600:a7cd:7757:1758:28a8.

23. Tziotis D, Hertkorn N, Schmitt-Kopplin P. 2011. Kendrick-analogous network visualisation of ion cyclotron resonance fourier transform mass spectra: improved options for the assignment of elemental compositions and the classification of organic molecular complexity. Eur J Mass Spectrom (Chichester) 17:415–421. https://doi.org/10.1255/ejms.1135
24. Herzsprung P, von Tümpling W, Hertkorn N, Harir M, Büttner O, Bravidor J, Friese K, Schmitt-Kopplin P. 2012. Variations of DOM quality in inflows of a drinking water reservoir: linking of van Krevelen diagrams with EEMF spectra by rank correlation. Environ Sci Technol 46:5511–5518. https://doi.org/10.1021/es300345c
25. Handle F, Harir M, Füssl J, Koyun AN, Grossegger D, Hertkorn N, Eberhardsteiner L, Hofko B, Hospodka M, Blab R, Schmitt-Kopplin P, Grothe H. 2017. Tracking aging of bitumen and its saturate, aromatic, resin, and asphaltene fractions using high-field fourier transform ion cyclotron resonance mass spectrometry. Energy Fuels 31:4771–4779. https://doi.org/10.1021/acs.energyfuels.6b03396
26. Michas A, Harir M, Lucio M, Vestergaard G, Himmelberg A, Schmitt-Kopplin P, Lueders T, Hatzinikolaou DG, Schöler A, Rabus R, Schloter M. 2020. Sulfate alters the competition among microbiome members of sediments chronically exposed to asphalt. Front Microbiol 11:556793. https://doi.org/10.3389/fmicb.2020.556793
27. Harir M, Cawley KM, Hertkorn N, Schmitt-Kopplin P, Jaffé R. 2022. Molecular and spectroscopic changes of peat-derived organic matter following photo-exposure: effects on heteroatom composition of DOM. Sci Total Environ 838:155790. https://doi.org/10.1016/j.scitotenv.2022.155790
28. Valle J, Harir M, Gonsior M, Enrich-Prast A, Schmitt-Kopplin P, Bastviken D, Hertkorn N. 2020. Molecular differences between water column and sediment pore water SPE-DOM in ten Swedish boreal lakes. Water Res 170:115320. https://doi.org/10.1016/j.watres.2019.115320
29. Cho Y, Birdwell JE, Hur M, Lee J, Kim B, Kim S. 2017. Extension of the analytical window for characterizing aromatic compounds in oils using a comprehensive suite of high-resolution mass spectrometry techniques and double bond equivalence versus carbon number plot. Energy Fuels 31:7874–7883. https://doi.org/10.1021/acs.energyfuels.7b00962
30. He Y, Hu Y, Huang H, Zeng H, Ni J, Dong H, Zhang F, She Y. 2023. Dynamic variations of oil components and microbial communities during indigenous microbial stimulation pilot study in low-permeability reservoirs. Energy Reports 9:5155–5165. https://doi.org/10.1016/j.egyr.2023.04.102
31. Annweiler E, Michaelis W, Meckenstock RU. 2001. Anaerobic cometabolic conversion of benzothiophene by a sulfate-reducing enrichment culture and in a tar-oil-contaminated aquifer. Appl Environ Microbiol 67:5077–5083. https://doi.org/10.1128/AEM.67.11.5077-5083.2001
32. Safinowski M, Griebler C, Meckenstock RU. 2006. Anaerobic cometabolic transformation of polycyclic and heterocyclic aromatic hydrocarbons: evidence from laboratory and field studies. Environ Sci Technol 40:4165–4173. https://doi.org/10.1021/es0525410
33. Jobelius C, Ruth B, Griebler C, Meckenstock RU, Hollender J, Reineke A, Frimmel FH, Zwiener C. 2011. Metabolites indicate hot spots of biodegradation and biogeochemical gradients in a high-resolution monitoring well. Environ Sci Technol 45:474–481. https://doi.org/10.1021/es1030867
34. Kuhn EP, Suflita JM. 1989. Microbial degradation of nitrogen, oxygen and sulfur heterocyclic compounds under anaerobic conditions: studies with aquifer samples. Environ Toxicol Chem 8:1149–1158. https://doi.org/10.1002/etc.5620081207
35. Yamada-Onodera K, Mukumoto H, Katsuyaya Y, Saiganji A, Tani Y. 2001. Degradation of polyethylene by a fungus, *Penicillium simplicissimum* YK. Polym Degrad Stab 72:323–327. https://doi.org/10.1016/S0141-3910(01)00027-1
36. Qian K, Robbins WK, Hughey CA, Cooper HJ, Rodgers RP, Marshall AG. 2001. Resolution and Identification of elemental compositions for more than 3000 crude acids in heavy petroleum by negative-ion microelectrospray high-field fourier transform ion cyclotron resonance mass spectrometry. Energy Fuels 15:1505–1511. https://doi.org/10.1021/ef010111z
37. Wilkes H, Schwarzbauer J. 2010. Hydrocarbons: an introduction to structure, physico-chemical properties and natural occurrence, p 1–48. In Timmis KN (ed), Handbook of hydrocarbon and lipid microbiology. Springer Berlin Heidelberg, Heidelberg.
38. Korenblum E, Souza DB, Penna M, Seldin L. 2012. Molecular analysis of the bacterial communities in crude oil samples from two brazilian offshore petroleum platforms. Int J Microbiol 2012:156537. https://doi.org/10.1155/2012/156537
39. Voskuhl L, Akbari A, Müller H, Pannekens M, Brusilova D, Dyksma S, Haque S, Graupner N, Dunthorn M, Meckenstock RU, Brauer VS. 2021. Indigenous microbial communities in heavy oil show a threshold response to salinity. FEMS Microbiol Ecol 97:12. https://doi.org/10.1093/femsec/fiab157
40. Gieg LM, Fowler SJ, Berdugo-Clavijo C. 2014. Syntrophic biodegradation of hydrocarbon contaminants. Curr Opin Biotechnol 27:21–29. https://doi.org/10.1016/j.copbio.2013.09.002
41. Mbadinga SM, Wang L-Y, Zhou L, Liu J-F, Gu J-D, Mu B-Z. 2011. Microbial communities involved in anaerobic degradation of alkanes. Int Biodeterior Biodegradation 65:1–13. https://doi.org/10.1016/j.ibiod.2010.11.009
42. Kurth JM, Nobu MK, Tamaki H, de Jonge N, Berger S, Jetten MSM, Yamamoto K, Mayumi D, Sakata S, Bai L, Cheng L, Nielsen JL, Kamagata Y, Wagner T, Welte CU. 2021. Methanogenic archaea use a bacteria-like methyltransferase system to demethoxylate aromatic compounds. ISME J 15:3549–3565. https://doi.org/10.1038/s41396-021-01025-6
43. Zhou Z, Zhang C, Liu P, Fu L, Laso-Pérez R, Yang L, Bai L, Li J, Yang M, Lin J, Wang W, Wegener G, Li M, Cheng L. 2022. Non-syntrophic methanogenic hydrocarbon degradation by an archaeal species. Nature 601:257–262. https://doi.org/10.1038/s41586-021-04235-2
44. Ihssen J, Egli T. 2005. Global physiological analysis of carbon- and energy-limited growing *Escherichia coli* confirms a high degree of catabolic flexibility and preparedness for mixed substrate utilization. Environ Microbiol 7:1568–1581. https://doi.org/10.1111/j.1462-2920.2005.00846.x
45. Heker I, Seitz C, Voskuhl L, Kong Y, Erdmann I, Götz F, Hassoun M, Huber C, Eisenreich W, Meckenstock RU. 2025. Chemoorganoautotrophic lifestyle of the anaerobic enrichment culture N47 growing on naphthalene. Commun Biol 8:856. https://doi.org/10.1038/s42003-025-08172-y
46. Meckenstock RU, Annweiler E, Michaelis W, Richnow HH, Schink B. 2000. Anaerobic naphthalene degradation by a sulfate-reducing enrichment culture. Appl Environ Microbiol 66:2743–2747. https://doi.org/10.1128/AEM.66.7.2743-2747.2000